

# Correlation of Magnus Force Data for Slender Spinning Cylinders

JAMES D. IVERSEN\*

*Iowa State University, Ames, Iowa*

Time-dependent results of numerical finite-difference solution for the two-dimensional spinning circular cylinder are used to derive a correlation parameter for analysis of experimental Magnus force data. The correlation parameter, which is a function of angle of attack, the fineness ratio, and the Reynolds number, is derived on the basis of the impulse or cross-flow analogy. The correlation parameter, derived for finless slender spinning circular cylinders is shown to successfully correlate experimental data for fineness ratios from 6 to 24, for subsonic through supersonic freestream speeds, and for cross-flow Mach numbers up to 0.4 at transonic and supersonic speeds.

## Nomenclature

- $c_l$  = two-dimensional lift coefficient, lift per unit span/(1/2) $\rho U_c^2 d$   
 $C_y$  = local side-force coefficient, side-force per unit span/(1/2) $\rho U_c^2 d$   
 $C_{y_p}$  = Magnus force coefficient,  $8Y/\rho U_\infty^2 \pi d^2 \hat{p}$   
 $d$  = body diameter  
 $k$  = constant of proportionality  
 $l$  = body length  
 $M_\infty$  = freestream Mach number  
 $p$  = spin rate  
 $\hat{p}$  = dimensionless spin rate,  $pd/2U_\infty$   
 $t$  = time  
 $U_\infty$  = freestream speed  
 $U_c$  = component of freestream speed normal to body axis  
 $V$  = tangential surface speed due to spin  
 $x$  = distance along body axis from nose  
 $Y$  = Magnus force  
 $\alpha$  = angle of attack  
 $\nu$  = kinematic viscosity  
 $\rho$  = air density

## Introduction

THE lateral aerodynamic force acting on a body of revolution due to a combination of angle of attack and axial spin rate, known as the Magnus force<sup>1</sup> has long been a source of difficulty to those who have attempted to measure or predict its value. The magnitude of the Magnus coefficient  $C_y$  is known to be a highly variable function of the boundary-layer character (laminar or turbulent), the nose and base shapes and discontinuities in streamline shape, as well as angle of attack, fineness ratio, spin rate, and the Reynolds and Mach numbers.<sup>2,3</sup>

The Magnus force, while small in magnitude compared to the normal force, can significantly affect the flight trajectory of a slender projectile.<sup>4</sup> Because of the difficulty in estimating the Magnus force and in measuring it experimentally, a new correlation parameter is presented with which the experimental values of Magnus force on slender finless spinning circular cylinders can be correlated. The correlation parameter is derived by using time-dependent results of numerical finite-difference solution in the cross-flow analogy. Although the presence of fins is not considered, the effect of the body boundary layer and vortex wake structure on the Magnus force contribution from the fins on a finned body is large,<sup>5</sup> and increased understanding of the body contribution may lead to more accurate analyses of fin effects.

## Boundary-Layer Analyses

The boundary layer on a streamlined body of revolution, for zero spin and for angles of attack smaller than necessary for lee-side separation to occur, would be symmetrical with respect to the angle-of-attack plane. With finite spin, however, the boundary-layer structure becomes asymmetric. The effective aerodynamic shape of the body, formed by the displacement thickness surface, is no longer symmetric with respect to the angle-of-attack plane, and an out-of-plane, or Magnus, force can occur.

Martin<sup>6</sup> calculated the laminar boundary layer on the spinning cylinder at low angle of attack, and used slender-body theory to calculate the Magnus force due to asymmetric displacement thickness growth. Kelly<sup>7</sup> added the effects of skin friction and radial pressure gradient and later Kelly and Thacker<sup>8</sup> considered higher-order terms in spin to account for nonlinear effects of spin. Their result for magnus coefficient is

$$C_{y_p} = - \left[ 8\alpha(l/d)^2 \left( \frac{U_\infty l}{\nu} \right)^{1/2} \right] [7.834 - 16.526(\hat{p})^2(l/d)^2] \quad (1)$$

and for center of pressure location is

$$\bar{x}/l = 0.600 - 0.375(\hat{p})^2(l/d)^2 \quad (2)$$

Martin's result<sup>6</sup> or the first term in Eq. (1) agrees fairly well for short bodies with laminar boundary layers for very small angles of attack.<sup>2</sup> Martin also suggested that for turbulent boundary layers the displacement thickness, and therefore the Magnus coefficient, would be a weaker function of Reynolds number (negative one-fifth power rather than negative one-half power). Although the Magnus coefficient magnitude often decreases at higher spin rates, at least at subsonic speeds,<sup>9</sup> as indicated by the second term in Eq. (1), it does not decrease at the large rate predicted by the second term of Eq. (1).

## Magnus Force at Higher Angles of Attack

Acyclic potential flow outside of the boundary layer (in accordance with Kelvin's circulation theorem) was assumed in the derivation of Eq. (1). For higher angles of attack, separation occurs and vorticity is shed into the wake region above the cylinder. Due to spin, the amounts of vorticity shed into the wake from either side of the cylinder are not equal; a circulation is developed about a lateral loop enclosing the cylinder, and the Magnus force increases to values higher than that predicted by the boundary-layer theory of Eq. (1). Smoke tunnel photographs of a spinning body clearly show the asymmetric vortex pattern.<sup>10</sup>

If the amount of developed circulation as a function of distance along the body axis was known, then the Magnus force could be predicted. Unfortunately, as Moore<sup>11</sup> points out, it is in general not possible to solve for circulation without complete solution of the Navier-Stokes equations. An additional complicating factor for high-fineness-ratio bodies is the possibility of side-force at high

Received September 8, 1972; also presented as Paper 72-966 at the AIAA 2nd Atmospheric Flight Mechanics Conference, Palo Alto, Calif., September 11-13, 1972; revision received November 20, 1972. This research was supported by the ISU Research Foundation and the Engineering Research Institute, Iowa State University.

\* Professor, Department of Aerospace Engineering, Engineering Research Institute and Aerospace Engineering. Member AIAA.

angle of attack even without spin due to an asymmetric vortex pattern consisting of vortices shed alternately from either side of the cylinder.<sup>5,12</sup>

### The Cross-Flow Analogy

Calculation of aerodynamic forces on a slender body at angle of attack in the plane containing the body axis and the free-stream velocity vector by considering the cross flow as an equivalent two-dimensional incompressible steady or unsteady problem has led to useful results many times. Munk<sup>13</sup> applied two-dimensional potential flow theory to determine the forces on airships, and later, Jones<sup>14</sup> studied the development of lift on a low-aspect-ratio pointed wing.

Experience has shown that the calculated value of lift, according to Munk's formula for bodies of revolution, is exceeded by the experimental value by an amount which increases proportional to the angle of attack. Allen<sup>15</sup> thus proposed a corrective addition to the lift to account for viscous effects, i.e., the cross-flow drag, which accounts for increase in both lift and drag of the body. Kelly,<sup>16</sup> in turn, suggested an improvement to Allen's use of a constant cross-flow drag coefficient by employing the time-dependent drag experienced by a cylinder started impulsively from rest,<sup>17</sup> where the time  $t$  in the time-dependent two-dimensional cylinder case is replaced by  $x/U_\infty \cos \alpha$  for the slender inclined body of revolution. The progressive development of the flow in the cross-flow analogy when viewed in the cross-flow plane which moves from the nose with speed equal to the axial component of freestream speed, is assumed to be similar to the time-dependent growth of flow about a two-dimensional cylinder started impulsively from rest.

The use of the cross-flow analogy to predict the Magnus force on a slender-inclined spinning body has been suggested previously.<sup>2,18,19</sup> Unfortunately, as pointed out by Platou,<sup>2</sup> no time-dependent experimental data for a spinning cylinder impulsively started from rest, two-dimensional or otherwise, has been available, and use of the steady Magnus force on the two-dimensional cylinder in the cross-flow analogy results in a grossly overestimated Magnus force prediction, except for cross-flow Mach numbers of 0.8 or higher.<sup>2</sup> A small amount of data from a time-dependent numerical experiment<sup>20</sup> using a finite-difference procedure has recently become available, however, and is used here to derive a new parameter for use in the correlation of experimental data.

### Time-Dependent Force on Two-Dimensional Cylinders and Its Use in the Cross-Flow Analogy

Thoman and Szweczyk<sup>20</sup> have recently calculated the time-dependent flowfield for flow normal to the axis of a two-dimensional circular cylinder rotated impulsively from rest. They present streamline patterns for surface to freestream speed ratios  $V/U_c$  of 2, 4, 6, for Reynolds numbers  $U_c d/\nu$  of 30, 200 and 40,000 and for various values of the dimensionless time  $U_c t/d$ . Values of time-dependent lift coefficient, estimated from Thoman and Szweczyk's results correlate very well by means of the following relationship

$$C_l = f \left\{ \frac{U_c t}{d} \left( \frac{V}{U_c} \right) \left( \frac{U_c d}{\nu} \right)^{1/4} \right\} \quad (3)$$

In the cross-flow analogy for slender spinning bodies of revolution the corresponding expression for the above correlation parameter can be used to obtain a functional relationship for the Magnus force coefficient  $C_{y_p}$ . The dimensionless parameters in the cross-flow analogy corresponding to  $U_c t/d$ ,  $V/U_c$  and  $U_c d/\nu$

$$U_c t/d = (U_\infty \sin \alpha / d)(x/U_\infty \cos \alpha) = (x/d) \tan \alpha \quad (4)$$

$$V/U_c = p d / 2 U_\infty \sin \alpha = \hat{p} / \sin \alpha \quad (5)$$

$$U_c d/\nu = (U_\infty \sin \alpha) d / \nu = (U_\infty d / \nu) \sin \alpha \quad (6)$$

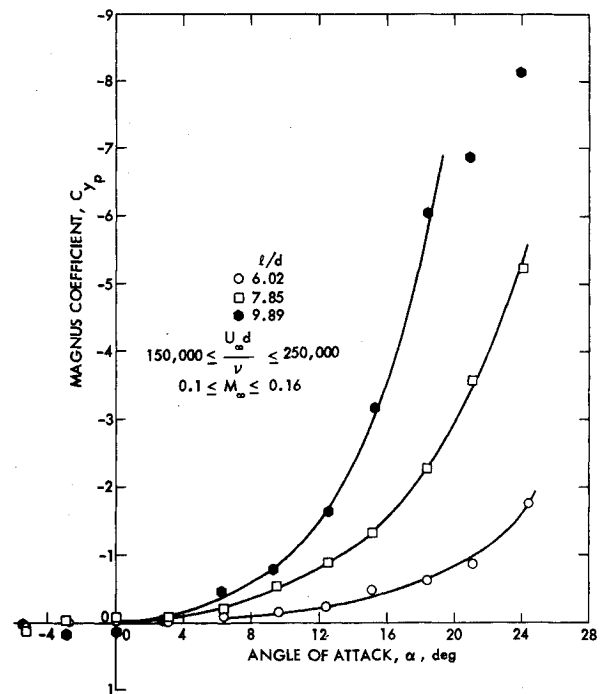


Fig. 1 Magnus force coefficient vs angle of attack.

The correlation parameter in Eq. (3), in terms of the slender spinning body at small angle of attack becomes

$$C_y = f \left[ \frac{x}{d} \hat{p} \tan \alpha \sin^{-5/4} |\alpha| \left( \frac{U_\infty d}{\nu} \right)^{1/4} \right] \quad (7)$$

where in Eq. (7) the side-force coefficient  $C_y$  is a local value and is a function of the distance  $x$  from the nose. It is now assumed, for small values of the functional parameter in Eq. (7), that the local side-force coefficient is linearly proportional to the parameter, i.e.,

$$C_y = -k \frac{x}{d} \hat{p} \tan \alpha \sin^{-5/4} |\alpha| \left( \frac{U_\infty d}{\nu} \right)^{1/4} \quad (8)$$

The side-force coefficient  $C_y$  in Eqs. (7) and (8) is based on local projected side-area and the cross-flow dynamic pressure. The total side-force is obtained by integrating the side-force from the nose to the base of the body. The resulting expression for Magnus force coefficient is

$$C_{y_p} = -k \frac{2}{\pi} \left( \frac{l}{d} \right)^2 \tan \alpha \sin^{3/4} |\alpha| \left( \frac{U_\infty d}{\nu} \right)^{1/4} \quad (9)$$

This expression is derived for a constant diameter body, neglecting the effect of nose shape. The error involved for a long body with a short nose would be small since the contribution of the nose region to total force is small. The center of pressure for the Magnus force corresponding to Eq. (9) is two-thirds the distance from the nose to the base, a value which corresponds fairly well with experiments.

### Correlation of Experimental Data-Subsonic Speed

Subsonic wind-tunnel tests of a spinning 3-in.-diam body were conducted at the Iowa State University Aerodynamics Lab. The nose shape of the model is a sphere-cone faired into the cylindrical afterbody. Experimental data for dimensionless spin rates of from -0.35 to +0.35 are shown in Fig. 1. The Magnus force coefficient is a strong function of fineness ratio  $l/d$ , as is well known.

The same experimental data are replotted in Fig. 2 as a function of the correlation parameter of Eq. (9). The data for the two

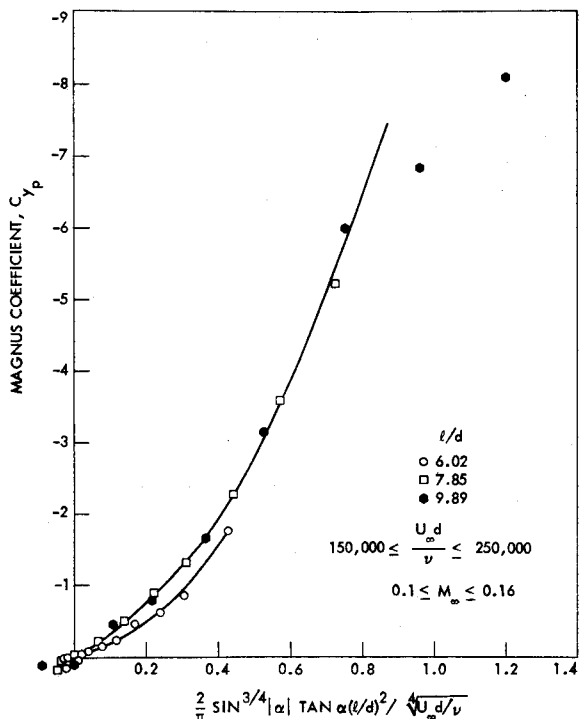


Fig. 2 Magnus force coefficient vs cross-flow analogy parameter.

higher fineness ratios correlate very well. The data for the smallest fineness ratio do not quite correspond, as might be expected, since the approximations of equivalent two-dimensional flow in the cross-flow analogy are more appropriate for the long, higher fineness-ratio bodies.

Subsonic data from Luchuk and Sparks' experiments<sup>21</sup> are replotted as a function of the cross-flow analogy correlation parameter in Fig. 3. The data replotted here represent spin ratios of up to 250 rps. Above that value, their data show decreases in the slope of the  $C_y$  vs  $p$  curves. An examination of other data at subsonic speeds, for example, in Hauer and Kelly<sup>9</sup> and in Greene<sup>3</sup> also shows a change in slope. As reported by a number of investigators, and summarized by Swanson<sup>22</sup> the steady Magnus force exhibited by the two-dimensional spinning cylinder is not linearly proportional to the speed ratio  $V/U_c$ . Therefore, it

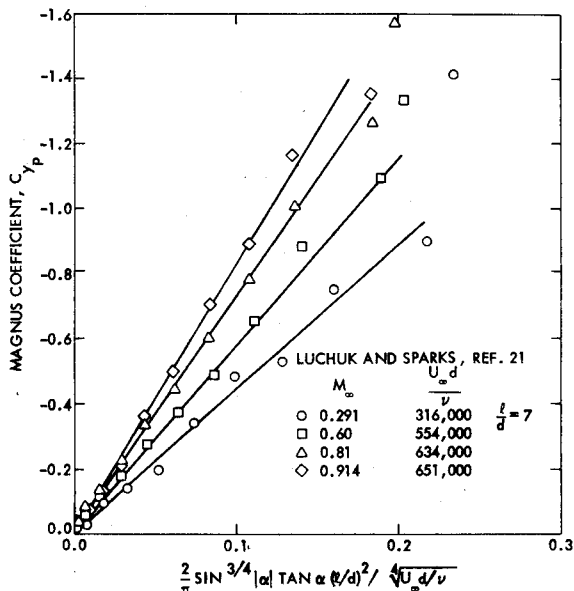


Fig. 3 Magnus force coefficient vs cross-flow analogy parameter.

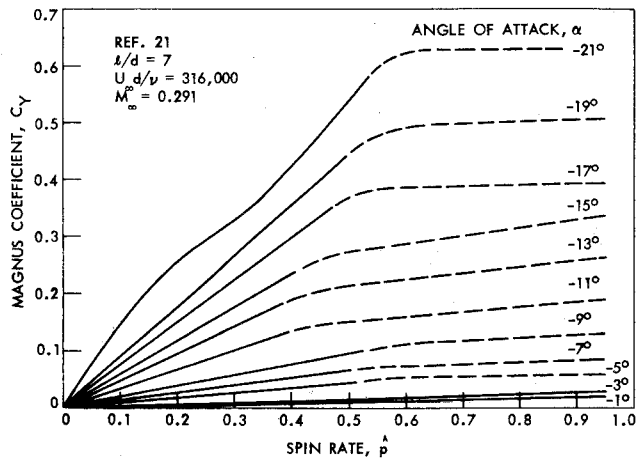


Fig. 4 Side force coefficient vs spin rate.

might be expected that the assumption of linearity inherently assumed in Eqs. (3, and 7-9) is not always correct. A more general correlation expression allowing for nonlinearity is given in Eq. (10):

$$C_{Yp} = f \left[ \frac{\hat{p}}{\sin \alpha}, \frac{1}{\pi} \frac{\sin^{7/4} |\alpha| \tan \alpha [l/d]^2}{\left( \frac{U_{\infty} d}{\nu} \right)^{1/4}} \right] \quad (10)$$

In this expression, the ratio of the surface to cross-flow velocity is assumed an important parameter in the cross-flow analogy as it is in the steady-state two-dimensional case. Actually, in the steady-state two-dimensional situation, the Magnus lift coefficient is also a strong function of Reynolds number for speed ratios below 0.5, and can even be negative for certain values of speed-ratio and Reynolds number.<sup>23,24</sup> For the spinning body of revolution at low angle of attack, however, although negative forces are sometimes observed, the effects of the axial component of the boundary layer and the time-dependence of the flow as it moves from the nose combine to alter the physical picture. The correlation parameter of Eq. (9) appears to be valid for small values of the parameter at subsonic speeds.

The Magnus coefficient,  $C_{Yp}$ , does decrease with spin rate for higher values of  $p$ , at least at subsonic speeds. Figures 4 and 5 present Luchuk and Sparks' data<sup>21</sup> for  $M_{\infty} = 0.291$  which show the decrease in slope of the  $C_y$  vs  $\hat{p}$  curve for values of  $\hat{p}$  greater than 0.4. Figure 5 shows the effectiveness of the correlation in the linear spin range with all data, for magnitudes of  $\hat{p}$  and  $\alpha$  less

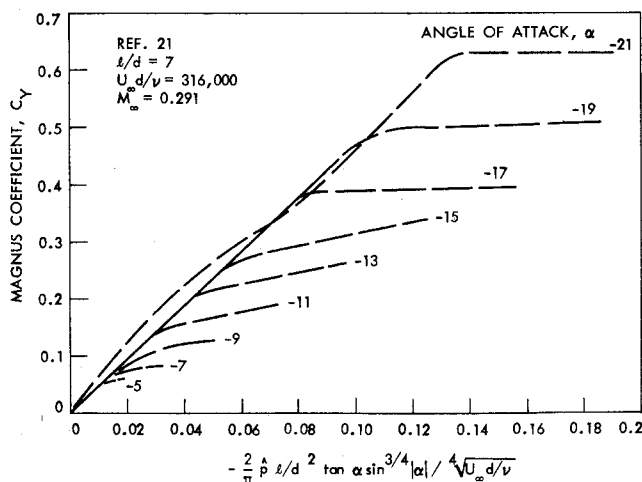


Fig. 5 Side force coefficient vs product of spin rate and cross-flow analogy parameter.

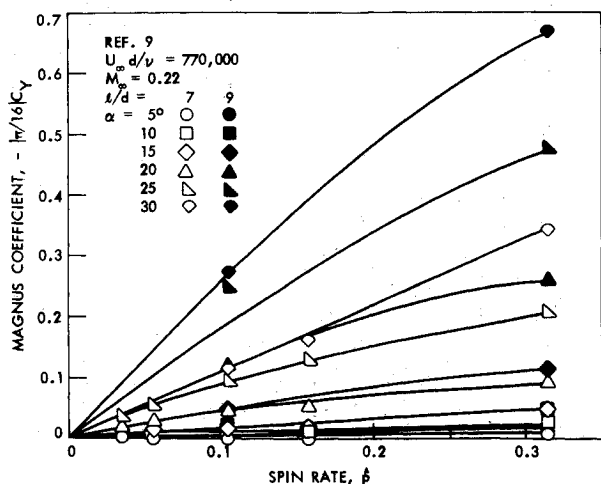


Fig. 6 Side force coefficient vs spin rate.

than 0.4 and  $21^\circ$ , respectively, falling on a single curve. The data of Hauer and Kelly,<sup>9</sup> however, also at low subsonic Mach number, show nonlinearity with spin throughout the range of spin rates tested, and the correlation as shown in Figs. 6 and 7 is not as good. Differences might be due to nose shape, which is conical in Figs. 6 and 7 and ogival in Figs 4 and 5. In both cases, the decrease in  $C_{yp}$  is much less than predicted by Eq. (1).

The large amount of scatter in the small amount of data which are available precludes an attempt to find the form of the correlation function of Eq. (10). At any rate, for the lower spin rates, Luchuk and Sparks' data at each subsonic Mach number appear to follow Eq. (9) quite well, as do all results at supersonic speeds as will be shown later. The constant  $k$  (slope of curves in Fig. 3) is seen to increase with increasing subsonic Mach number.

### Correlation of Experimental Data-Subsonic Speed

Figure 8 shows experimental data plotted from several sources<sup>5,21,25</sup> for spinning bodies at supersonic speeds. These data are replotted in Fig. 9 as a function of the cross-flow analogy parameter of Eq. (9). Except for the deviations, noted by the dotted lines, which are explained later, a remarkable degree of correlation exists, considering the range of Mach numbers and fineness ratios presented. In contrast to the subsonic case, neither the value of Mach number nor the value of spin rate seem to have any sensible effect on the correlation.

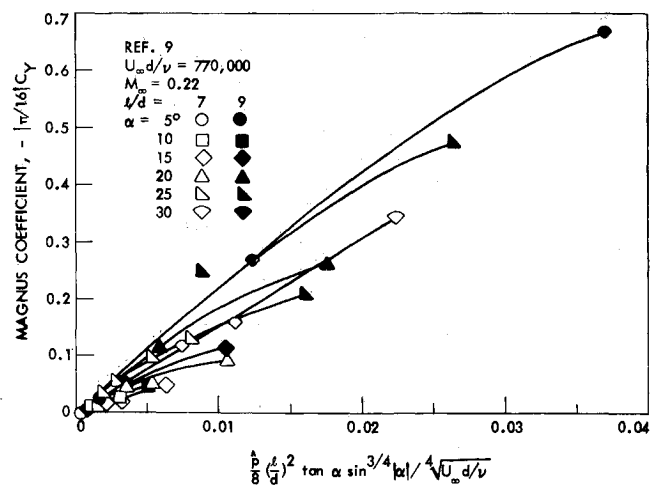


Fig. 7 Side force coefficient vs product of spin rate and cross-flow analogy parameter.

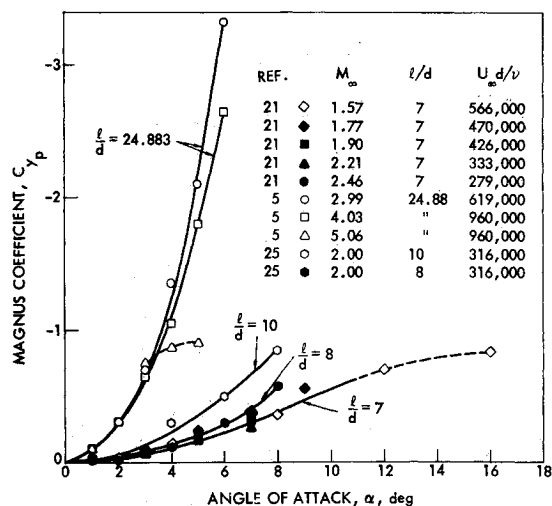


Fig. 8 Magnus force coefficient vs angle of attack.

There are limitations to the cross-flow analogy correlation which should be noted. As already indicated, the correlation should not be expected to hold for short bodies of low fineness ratio nor does it appear to be valid at higher spin rates for subsonic speeds. In addition, as Platou<sup>2</sup> notes, the Magnus force at intermediate angles of attack can be dependent on the cross-flow Mach number. The critical Mach number for flow normal to a spinning two-dimensional circular cylinder<sup>26</sup> is from 0.36 to 0.4. The angle of attack at which the cross-flow Mach number becomes 0.4 is given by

$$\alpha = \sin^{-1}(0.4/M_\infty) \quad (11)$$

Equation (11) is plotted in Fig. 10.

The typical  $C_{yp} - \alpha$  curve starts at a low angle of attack with a concave upward shape as in Figs 1 and 8. A maximum magnitude of Magnus force coefficient is reached at a sufficiently high angle of attack with, of course, an inflection point occurring at a slightly smaller angle. Data points from Refs. 3, 5, 9, 21 and 25 representing the angles of attack at which the inflection points and maximum values of  $C_{yp}$  occur are also plotted in Fig. 10. For transonic and supersonic freestream Mach numbers, Eq. (11) seems to represent an upper limit for the value of inflection point angle of attack and thus represents an upper limit for the validity of the cross-flow analogy correlation. The dashed portions of the curves in Figs. 8 and 9 do represent values of angle of attack higher than this limit and do as a result deviate from the correlation curve.

Platou<sup>2</sup> found an approximate correlation for data at high

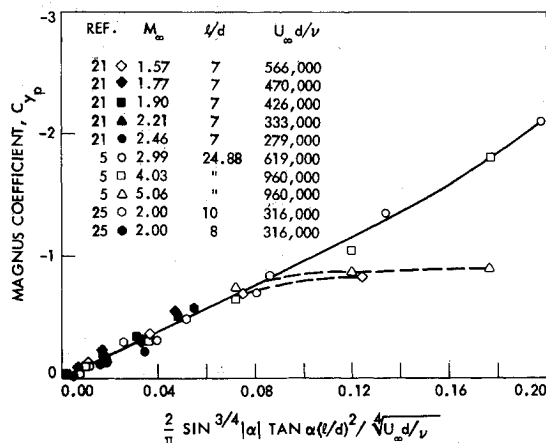


Fig. 9 Magnus force coefficient vs cross-flow analogy parameters.

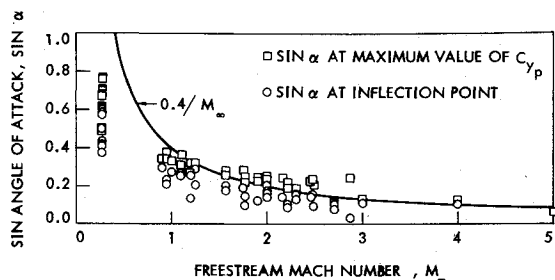


Fig. 10 Locations of maximum magnitude and inflection points on  $C^y - \alpha$  curves vs freestream Mach number.

angles of attack with steady-state data obtained on a spinning cylinder mounted normal to a transonic or supersonic stream. His correlation is approximately valid for cross-flow Mach numbers of 0.8 and higher. As he points out, when the cross flow is supersonic, circulation due to shed vorticity cannot develop over the entire cylinder, so that the effect of shed vorticity is restricted to the wake, thus the Magnus force is dependent at higher angles of attack on cross-flow Mach number. As noted earlier, for values of cross-flow Mach number less than 0.4, the Magnus force is independent of freestream Mach number at supersonic speeds.<sup>3</sup>

### Conclusions

A remarkable degree of correlation exists, especially at supersonic speeds, for Magnus force coefficient experimental data correlated by means of the cross-flow analogy parameter of Eq. (9). Data from the sphere-cone-cylinder tests (Figs. 1 and 2), and from Refs. 3, 5, 21 and 25 for bodies with ogival noses and from Ref. 9 for bodies with conical noses, cover the fineness ratio range from 5 to 24.88 and the Mach number range from 0.1 to 5.06. For all of these experiments, the value of the coefficient  $k$  in Eq. (9) ranges from approximately 5 to approximately 20. Most of the range in  $k$  appears to be attributable to differences in nose shape with a smaller change due to Mach number variation.

The cross-flow Mach number of 0.4 provides an angle of attack limitation to the correlation at transonic and supersonic free-stream speeds. At cross-flow Mach numbers of 0.8 and higher the cross-flow correlation of Platou<sup>2</sup> can be used to estimate the Magnus force coefficient.

### References

- <sup>1</sup> Magnus, G., "Ueber die Verdichtung der Gase an der Oberfläche glatter Körper," *Poggendorf, Annalen der Physik Chemie*, Vol. 88, 1853, pp. 604-610.
- <sup>2</sup> Platou, A. S., "Magnus Characteristics of Finned and Non-Finned Projectiles," *AIAA Journal*, Vol. 3, No. 1, Jan. 1965, pp. 83-90.
- <sup>3</sup> Greene, J. E., "A Summary of Experimental Magnus Characteristics of a 7- and 5-Caliber Body of Revolution at Subsonic through Supersonic Speeds," NAVORD Rept. 6110, 1958, U.S. Naval Ordnance Lab., White Oak, Md.
- <sup>4</sup> Stone, G. W., "The Magnus Instability of A Sounding Rocket," *AIAA Journal*, Vol. 4, No. 9, Sept. 1966, pp. 1560-1565.
- <sup>5</sup> Uselton, J. C. and Carman, J. B., "A Study of the Magnus Effects on a Sounding Rocket at Supersonic Speeds," *Journal of Spacecraft and Rockets*, Vol. 8, No. 1, Jan. 1971, pp. 28-34.
- <sup>6</sup> Martin, J. C., "On Magnus Effects Caused by the Boundary Layer Displacement Thickness on Bodies of Revolution at Small Angles of Attack," *Journal of the Aeronautical Sciences*, Vol. 24, No. 6, June 1957, pp. 421-429.
- <sup>7</sup> Kelly, H. R., "An Analytical Method for Predicting the Magnus Forces and Moments on Spinning Projectiles," TM-1634, 1954, U.S. Naval Ordnance Test Station, China Lake, Calif.
- <sup>8</sup> Kelly, H. R. and Thacker, G. R., "The Effect of High Spin on the Magnus Force on a Cylinder at Small Angles of Attack," NAVORD Rept. 5036, 1956, U. S. Naval Ordnance Test Station, China Lake, Calif.
- <sup>9</sup> Hauer, H. J. and Kelly, H. R., "The Subsonic Aerodynamic Characteristics of Spinning Cone-Cylinders and Ogive-Cylinders at Large Angles of Attack," NAVORD Rept. 3529, 1955, U.S. Naval Ordnance Test Station, China Lake, Calif.
- <sup>10</sup> Ingram, C. W., Iuscardi, R. J., and Nicolaidis, J. D., "Effects of Rifling and N-Vanes on the Magnus Characteristics of Bodies of Revolution," AIAA Paper 72-970, Palo Alto, Calif., 1972.
- <sup>11</sup> Moore, D. W., "The Flow Past a Rapidly Rotating Circular Cylinder in a Uniform Stream," *Journal of Fluid Mechanics*, Vol. 2, Pt. 6, 1957, pp. 541-550.
- <sup>12</sup> Thomson, K. D. and Morrison, D. F., "The Spacing, Position and Strength of Vortices in the Wake from Slender Cylindrical Bodies at Large Incidence," WRE Rept. HSA25, 1969, Australian Dept. of Supply.
- <sup>13</sup> Munk, M. M., "The Aerodynamic Forces on Airship Hulls," Rept. 184, 1924, NACA.
- <sup>14</sup> Jones, R. T., "Properties of Low-Aspect Ratio Pointed Wings at Speeds Below and Above the Speed of Sound," Rept. 835, 1946, NACA.
- <sup>15</sup> Allen, H. J. and Perkins, E. H., "A Study of Effects of Viscosity on Flow over Slender Inclined Bodies of Revolution," Rept. 1048, 1951, NACA.
- <sup>16</sup> Kelly, H. R., "The Estimation of Normal-Force, Drag, and Pitching Moment Coefficients for Blunt-Based Bodies of Revolution at Large Angles of Attack," *Journal of the Aeronautical Sciences*, Vol. 21, Aug. 1954, p. 549.
- <sup>17</sup> Schwabe, M., "Pressure Distribution in Non-Uniform Two-Dimensional Flow," Rept. TM 1039, 1943, NACA.
- <sup>18</sup> Buford, W. E., "Magnus Effect in the Case of Rotating Cylinders and Shell," BRL Memorandum Rept. 821, 1954, Ballistic Lab., Aberdeen Proving Ground, Md.
- <sup>19</sup> Fletcher, C. A. J., "Investigation of the Magnus Characteristics of a Spinning Inclined Ogive-Cylinder Body at  $M = 0.2$ ," WRE Rept. HSA 159, 1969, Australian Dept. of Supply.
- <sup>20</sup> Thoman, D. C. and Szweczyk, A. A., "Numerical Solutions of Time Dependent Two-Dimensional Flow of a Viscous Incompressible Fluid over Stationary and Rotating Cylinders," TR 66-14, 1966, Dept. of Mechanical Engineering, Univ. of Notre Dame, South Bend, Ind.
- <sup>21</sup> Luchuk, W. and Sparks, W., "Wind-Tunnel Magnus Characteristics of the 7-Caliber Army-Navy Spinner Rocket," NAVORD Rept. 3813, 1954, U.S. Naval Ordnance Lab., White Oak, Md.
- <sup>22</sup> Swanson, W. M., "The Magnus Effect: A Summary of Investigations to Date," *Journal of Basic Engineering*, Vol. 82, No. 9, Sept. 1961, p. 461.
- <sup>23</sup> Van Aken, R. W. and Kelly, H. R., "The Magnus Force on Spinning Cylinders," NAVORD Rept. 5583, 1957, U.S. Naval Ordnance Test Station, China Lake, Calif.
- <sup>24</sup> Krahn, E., "Negative Magnus Force," *Journal of the Aeronautical Sciences*, Vol. 23, 1956, p. 377.
- <sup>25</sup> Holmes, J. E., Regan, F. J., and Falusi, M. E., "Supersonic Wind Tunnel Magnus Measurements of the 7-, 8-, 9-, and 10-Caliber Army-Navy Spinner Projectile," NOLTR 68-172, 1968, U.S. Naval Ordnance Lab., White Oak, Md.
- <sup>26</sup> Heaslet, M. A., "Compressible Potential Flow with Circulation about a Circular Cylinder," Rept. 780, 1944, NACA.